THE EFFECT OF FLUID VISCOSITY IN T-SHAPED MICROMIXERS

Mina Roudgar, Elizabetta Brunazzi, Chiara Galletti and Roberto Mauri

Department of Chemical Engineering, Industrial Chemistry and Materials Science, University of Pisa
Via Diotisalvi 2, 56126 Pisa, Italy

Keywords: Micromixers, CFD.

Abstract: Effective mixing in small volumes is a crucial step in many chemical and biochemical processes, where microreactors are to ensure a fast homogenization of the reactants. Physically, liquid flows in microfluidic channels are characterized by low values of the Reynolds number and, in general, large values of the massive Peclet number. Accordingly, since general strategies of flow control in microfluidic devices should not depend on inertial effects, reduction of the mixing length requires that there must be transverse flow components. In this paper, three-dimensional numerical simulations were performed to study the flow dynamics and mixing characteristics of liquids flows inside T-shaped micromixers, when the two inlet fluids are either both water or water and ethanol. In particular we showed that, contrary to what one could think beforehand, the mixing efficiency of water-ethanol systems is lower than the corresponding water-water case.

1 INTRODUCTION

Mixing two different fluids in a micromixer is one of the most basic and revealing case in the general subject of microfluidics. Due to the small size of the device, fluids flows are typically laminar, so that, in simple channels (i.e. with smooth walls), pressure driven flows are laminar and uniaxial, so that confluencing liquids tend to flow side by side and mixing between the two streams is purely diffusive.

To reduce the mixing length, we must induce transverse flow components that stretch and fold fluid volumes over the cross section of the channel. This can be achieved using active or passive mechanisms (Nguyen and Wu, 2005; Hessel et al., 2005) .In general, active micro-mixers use external energy sources, to induce transversal flows and thus enhance mixing processes, while passive micro-mixers usually achieve the same effect by using clever channel geometries to stir or laminate fluids without external disturbances.The operation of the passive micromixer is easier and simpler because of no additional moving parts or energy sources (Yang and Lin, 2006; Yang et al., 2005; Kim et al., 2004; Aubin et al., 2005; Wang and Yang, 2006; Wang et al., 2007).

The simplest designs of a passive micromixers are T- or Y-shapes. These micromixers are quite suitable to carry out basic fundamental studies to understand mixing at the microscale.

Most of the previous works on T- or Y- shape micromixers is directed towards analyzing mixing for a wide range of Reynolds numbers and finding various flow types. It is well known, that the mixing performance varies significantly with Reynolds number.

The present study focuses on the effect of the viscosity difference between the two inlet fluids on the mixing efficiency in T-type passive micro mixers for a range of the Reynolds numbers (1 -300). To do that, a commercial Computational Fluid Dynamic (CFD) code, FLUENT 6.3 by Ansys Inc., is used to solve the three-dimensional flow and mass transfer equations   in   the   proposed   geometrical configurations.

2 SIMULATION TECHNIQUE

2.1 Governing Equations

Consider two fluids converging into a T junction: the two inlet streams have at the same temperature, so that, as the heat of mixing has a negligible effect

here, we may assume that the process is isothermal. In general, density and viscosity are known functions of the composition, so that the governing equations are:

$$\frac{\partial \rho}{\partial t} + \rho \nabla \cdot \mathbf{v} = 0, \tag{1}$$

$$\rho(\dot{\mathbf{v}} + \mathbf{v} \cdot \nabla \mathbf{v}) + \nabla p = \nabla \cdot \left[\mu(\nabla \mathbf{v} + \nabla \mathbf{v}^+) \right] + \rho g, \tag{2}$$

$$\dot{c} + \nabla \cdot (\mathbf{v}c) = D\nabla^2 c. \tag{3}$$

Here, $\mathbf{v}$ denotes the velocity vector, ρ the fluid density, p the pressure, μ the viscosity, g the gravity acceleration, D the molecular diffusivity (which here is assumed to be constant) and c the concentration of one of the two inlet fluids. If the two fluids are identical, we can imagine adding a very small amount of contaminant, i.e. a dye, to one of the fluids (which therefore continue to have the same physical properties) and therefore c indicates the dye concentration.

As mentioned in the Introduction, the characteristics of the velocity and concentration fields can be described through the Reynolds and Peclet numbers,

$$N_{\text{Re}} = \frac{Ud}{\nu}; \qquad N_{Pe} = \frac{Ud}{D}, \tag{4}$$

where U is the mean velocity, while the characteristic fluid length d is assumed to be the hydraulic diameter D_h, i.e.,

$$d = D_h = \frac{2WH}{(W+H)}, \tag{5}$$

where W and H are the channel width and height, respectively (see Figure 1).

2.2 Characterization of the Degree of Mixing

Based on the above considerations, we will use a definition of mixing efficiency based on material fluxes, instead of concentration, as the former, not the letter, are conserved quantities. Accordingly, we define a cup mixing flow variance as:

$$\sigma_{cm}^2(x) = \frac{1}{A} \int_A \left[\frac{v(y,z)c(x,y,z)}{\overline{v}\overline{c}_{cm}} - 1 \right]^2 dydz$$

i.e.

$$\sigma_{cm}^2 = \frac{1}{N} \sum_{i=1}^{N} \left(\frac{v_i c_i}{\overline{v}\overline{c}_{cm}} - 1 \right)^2, \tag{6}$$

where $\overline{v}\overline{c}_{cm}$ is the (constant) contaminant flux.

For sake of convenience, here we will use the following definition of degree of mixing,

$$\delta_m = 1 - \sigma_{cm} \tag{7}$$

We expect that δ_m increases monotonically with x, tending asymptotically to 1 as the two fluids mix completely.

2.3 The Inlet Velocity Profile and the Mixing Zone

The fully developed velocity profile in a closed rectangular conduit can be easily obtained by solving the Navier-Stokes equations with no-slip boundary conditions at the walls and a constant axial pressure gradient G. For our purposes, the most convenient form of this solution is (Chatwin and Sullivan, 1982):

$$v(y,z) = -\frac{G}{2\mu} y(Y-y) - \frac{4GY^2}{\mu \pi^3} \sum_{k \; odd} \frac{1}{k^3} \tag{8}$$
$$\sin\left(k\pi \frac{y}{Y}\right)\left[Cosh\left(k\pi \frac{z}{Y}\right) - Tanh\left(\frac{k\pi}{2\eta}\right)Sinh\left(k\pi \frac{z}{Y}\right)\right]$$

where Y and Z are the sizes of the conduit, while $\eta = Y/Z$ is the aspect ratio.

From this expression, we can derive the pressure gradient G as a function of mean velocity $\overline{v}$, finding:

$$G = -\frac{12\mu \overline{v}}{Y^2} \left[1 - \frac{192}{\pi^5} \eta \sum_{k \; odd} \frac{1}{k^5} Tanh\left(\frac{k\pi}{2\eta}\right) \right]^{-1} \tag{9}$$

We have assumed that the velocity profile remains fully developed, and therefore given by the above expression, up to a certain distance from the T junction, where the influence of vortices and engulfment of the mixing zone starts to be felt. For the value of this distance, we used the results given by Soleymani et al. (2009); who determined it by numerical simulation.

3 RESULTS AND DISCUSSION

3.1 Numerical Scheme

The geometric setting of our simulation, as shown in Figure 1, is identical to the one used by Bothe (2006), with two *100μm×100μm* inlet square channels and a *200μm×100μm* mixing channel. The simulations were conducted using 2.5 *μm* body-fitted structured grids in all directions, created by GAMBIT.

At the walls, no-slip and no-mass-flux boundary conditions were applied, while mass flow rates with uniform velocity and uniform concentration fields, were imposed at the entrances. In addition, a condition of average pressure outlet was set at the exit of the micromixer. A second order discretization scheme was used to solve all equations, using FLUENT 6.3 by Ansys Inc.

Simulation were typically considered converging when the normalized residuals for velocities fell below 1×10^{-6}.
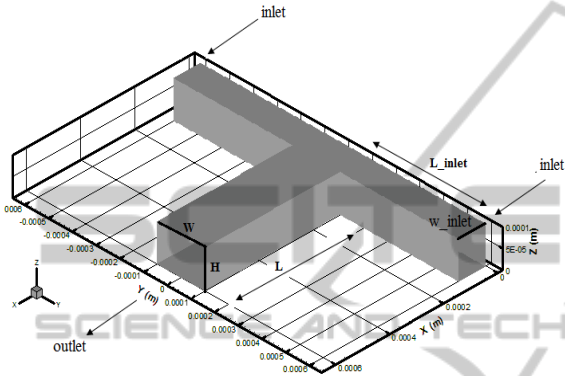
Figure 1: Schematics of the T-mixer.

The values of density and viscosity were set equal to 10^3 kg m^{-3} and 10^{-3} kg m^{-1} s^{-1} for water and 789 kg m^{-3} and 1.2×10^{-3} kg m^{-1} s^{-1} for ethanol, respectively , while the diffusion coefficient was set equal to $D = 3.23 \times 10^{-10}$ m^2 s^{-1}, corresponding to that of a water - ink mixture , as this value is very close to the self- diffusivity of pure water and of ethanol as well.

In our simulations, we compared the water-water case with the water-ethanol case, presenting them side by side.

3.2 Equal Inlet Velocity

At small flow rates, as wall shear stresses are small, the two streams behave in the same way, so that the velocity profile is symmetric along the y-direction (i.e. along channel width), both near the walls and at the center of the conduit (see Figure 2 , 3.a and 3.e). In fact, at small Reynolds number ($Re<30$), the flow patterns in water-water systems is very similar to those in water-ethanol systems, so that mixing occurs mainly by mass diffusion and it is therefore very slow rates with uniform velocity and uniform concentration fields, were imposed at the entrances. In addition, a condition of average pressure outlet was set at the exit of the micromixer.

By increasing the Reynolds number, we see
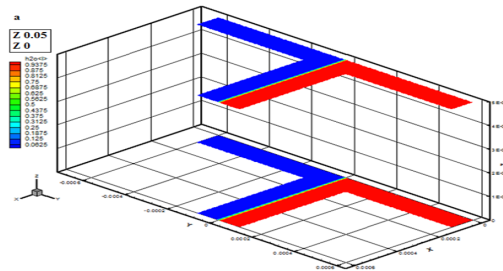
Figure 2: Mass fraction contour plot at $Re = 10$ for a water-ethanol system along the mixing channel close to the wall and at the channel center.

changes in the flow patterns. In fact, to compensate for its larger viscosity, ethanol moves slower than water, so that the pressure drops of the two fluid streams are equalized. This causes the water moving to the channel center, while ethanol is driven to the walls. This phenomenon is more evident when we move from the channel center to the walls, because of higher wall shear stresses (see Figure 3.b and 3.f). Note that the different residence times of the two fluids does not favor mixing by diffusion in the y-direction and hence the water-ethanol degree of mixing in smaller than its water-water counterpart. At further higher Reynolds numbers, we saw significant difference in flow patterns and degree of mixing because of the appearance of the vortices an engulfment. In fact, as we see in Figure 3.c and 3. d, in water-water systems, as we move from $Re = 100$ to $Re = 200$, we see the appearance of symmetric vortices and engulfment flows, thus confirming the results by Bothe (2006). On the other hand, as shown in Figure 3.g, 3.h and 3.i for water–ethanol systems the onset of the engulfment regime occurs at a higher Reynolds number, between. Concomitantly, in table 1 we see that the two systems exhibit a very large difference in the degree of mixing δ_m and wall shear stresses at the outlet of the micro T-mixer.

3.3 Unequal Inlet Velocity

Our simulation shows that when the two inlet streams have different velocities (and flow rates as well), the mixing process is radically different, depending on whether the majority fluid is water or ethanol. First, let us consider the behavior of a water-water system. At low Reynolds number, when the velocity of the two streams are different from each other, in Figures 4.a and 4.c we see that, as expected, the interface moves towards one of the walls, where the velocity is lower than that at the centerline (which corresponds to the velocity experienced by the interface region in the equal
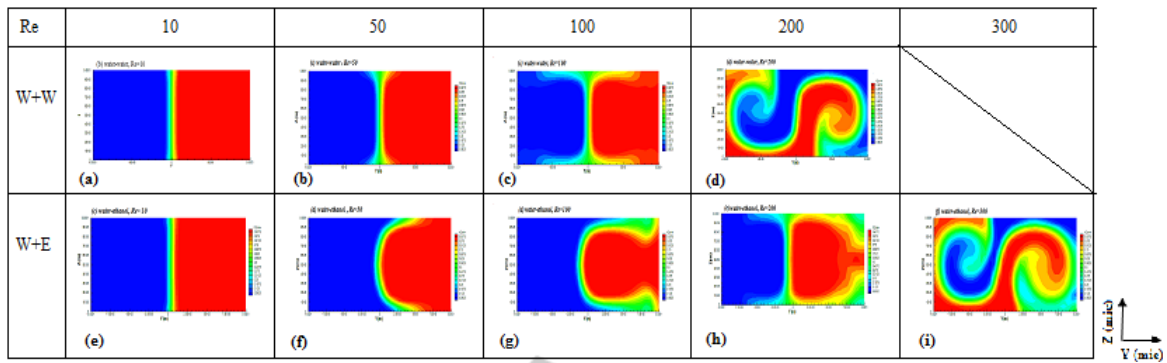
Figure 3: Mass fraction contour plot at different Reynolds number for water-water and b water-ethanol systems at the outlet cross section.

Table 1: Degree of mixing δ_m and wall shear stresses at the outlet of the micro T-mixer for water-water and water-ethanol systems at different Reynolds numbers.

| Re_{mix} | W+W | | | W+E | | | | |
| | $\sigma\%$(mixing efficiency) | τ(shear stress, mixing)(Pa) | | $\sigma\%$ | τ(inlet channel) | | τ(mixing channel) | |
		τ_0 (z=0)	τ_c(center)		τ_{0Water}	$\tau_{0Ethanol}$	τ_0	τ_c
1	4	0.47	0.05	3.2	0.57	0.63	0.514	0.056
10	2	4.7	0.51	1.2	5.31	6.33	5.16	0.57
20	-	-	-	1.6	10.4	12.7	10	1.1
30	-	-	-	2	16.3	19.7	15.8	1.66
40	-	-	-	2.2	22.1	26	21.4	2.2
50	3.6	25	2.5	2.4	28	32.7	27	2.8
100	10	57.4	5.11	5.8	68.5	60	61	5.6
200	26.4	142	12	8.9	133	149	148.4	12
300	41			31	218	235	248	21
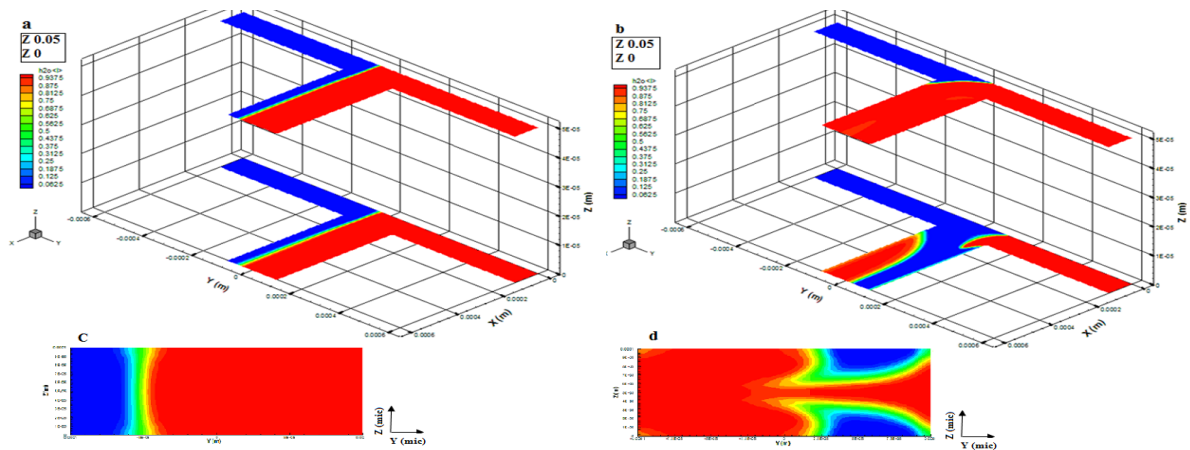
Figure 4: Mass fraction contour plots of water-water systems at a velocity ratio $V_1/V_2 = \beta = 5$ along the mixing channel (close to the wall and at the channel center) and at the outlet cross section for a) and c) $Re = 1$; c) and d) $Re = 100$.

velocity case). Accordingly, as the diffusion time is larger than that in the equal velocity case, the mixing degree increases also. Then, at larger Reynolds numbers, in Figures 4.b and 4.d we see that the faster fluid stream hops to the opposite side of the mixing channel, leaving the slower fluid close to the walls, resulting in an increase of a mixing efficiency. In water-ethanol systems, when the water stream is faster, we observe a behavior that is very similar to that of water-water systems, although, as shown in Table 2, the degree of mixing is smaller.
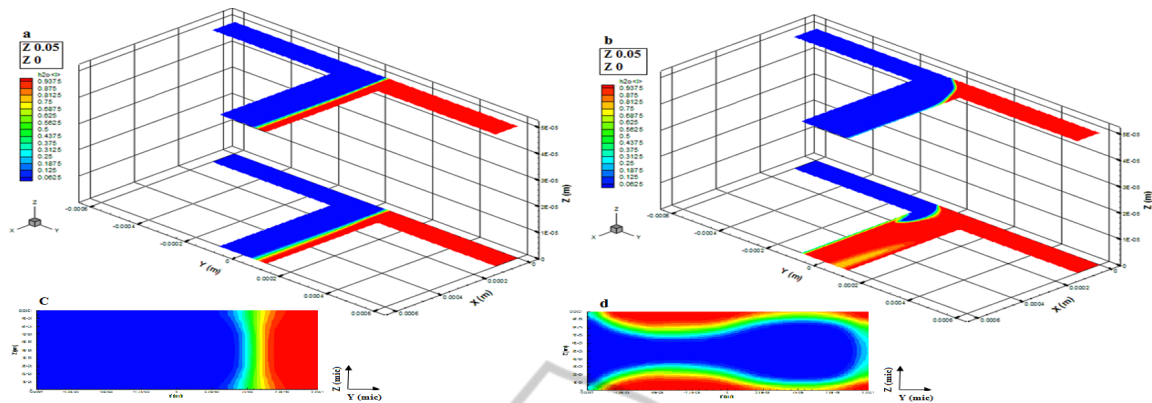
Figure 5: Mass fraction contour plots of water-ethanol systems at a velocity ratio $V_e/V_w = \beta = 5$ along the mixing channel (close to the wall and at the channel center) and at the outlet cross section for a) and c) *Re = 1*; c) and d) *Re = 100* .

On the other hand, for water-ethanol systems with ethanol being the faster stream, the behavior is radically different, as shown in Figure 7. In fact, in this case, comparing Fig. 4.d with 5.d, we see that at high Reynolds number, the faster stream, i.e. ethanol, now tends to hop to the opposite side even more easily, generating a phase pattern that is quite different. In addition, at low Reynolds number, comparing 4.c with 5.c, we see that the interface region is thicker and therefore the degree of mixing is higher. These observations are summarized in Table 2.

Table 2: Degree of mixing δ_m at the outlet of the micro T-mixer for water-water and water-ethanol systems at different Reynolds numbers and inlet velocity ratios.

Systems		W+W		W+E	
Re		1	100	1	100
σ%(mixing efficiency)	V1/V2=5	9.5	28	-	-
	Vw/Ve=5	-	-	5.7	23
	Ve/Vw=5	-	-	15.8	27

4 CONCLUSIONS

Three-dimensional numerical simulations were performed to study the flow dynamics and mixing characteristics of liquids flows inside T-shaped micromixers, when the two inlet fluids are either both water or water and ethanol. In particular we showed that, predictably, the degree of mixing is larger for unequal inlet flow rates. On the other hand, contrary to what one could think beforehand, the mixing efficiency of water-ethanol systems is lower than the corresponding water-water case.

REFERENCES

Nguyen, N. T., & Wu, Z. G., (2005). Micromixers-a review. *Journal of Micromechanics and Microengineering*, 15, R1–R16.

Hessel, V., Lowe, H., Schonfeld, F. (2005). Micromixers-a review on passive and active mixing principles. *Chemical Engineering Science*, 60, 2479– 2501.

Yang, J. T., & Lin, K. W. (2006). Mixing and separation of two-fluid flow in a micro planar serpentine channel. *Journal of Micromechanics and Microengineering*, 16, 2439–2448.

Yang, J. T., Huang, K. J., Lin, Y. C. (2005). Geometric effects on fluid mixing in passive grooved micromixers. *Lab on a Chip,* 5, 1140–1147.

Kim, D. S., Lee, S. W., Kwon, T. H., Lee, S. S. (2004). A barrier-embedded chaotic micromixer. *Journal of Micromechanics and Microengineering*, 14, 798–805.

Aubin, J., Fletcher, D. F., Xuereb, C. (2005). Design of micromixers using CFD modeling. *Chemical Engineering Science,* 60, 2503–2516.

Wang, L., & Yang, J. T. (2006) An overlapping crisscross micromixer using chaotic mixing principles. *Journal of Micromechanics and Microengineering,* 16, 2684–2691.

Wang, L., Yang, J. T., Lyu, P. C. (2007). An overlapping crisscross micromixer. *Chemical Engineering Science*, 62, 711–720.

Chatwin, P. C. & Sullivan, P. J. (1982). The effect of aspect ratio on the longitudinal diffusivity in rectangular channels. *Journal of Fluid Mechanic,* 120, 347-358.

Bothe, D., Sternich, C., Warnecke, H. J. (2006). Fluid mixing in a T-shaped micro-mixer. *Chemical Engineering Science*, 61, 2950–2958.

Lee, S., Lee, H. Y., Lee, I. F., Tseng, C.Y. (2004). Ink diffusion in water. *European Journal of Physics*, 25, 331–336.

Soleymani, A., Yousefi. H., Ratchananusorn, W., Turunen, I. (2010). Pressure drop in micro T-mixers. *Journal of Micromechanics and Microengineering*, 20, 015-029.